DC-Level Dimmable LED Driver With Primary Side On-Time Control for DC Distribution

Gab-Su Seo, *Student Member, IEEE*, Hye-Jin Kim, *Student Member, IEEE*, Kyu-Chan Lee, *Member, IEEE*, Sung-Jin Choi, *Member, IEEE*, and Bo-Hyung Cho, *Fellow, IEEE*

***Abstract*— This paper proposes a light-emitting diode (LED) lighting system using a dc-level dimming technique. This new dimming method realizes LED lamp control by having the LED drivers in the same zone recognize the level of their input voltage as a dimming signal with a dc-level dimmer and minimum communication interfaces. The proposed dc LED system also achieves improved system efficiency by matching the variable input voltage to the LED load conditions. Practical design guidelines for the LED driver circuit are presented for system implementation. The prototype circuit for a 24-W LED lamp is designed following the guidelines for verification. The proposed dc-level dimming system and the conventional dimming LED lighting system, which dispatches communication modules to individual drivers to obtain dimming signal, are implemented for a two-story parking lot and their performance is compared and evaluated. The experimental results of the prototype system show 6.8% energy saving compared with conventional lighting, which results from the improved driver efficiency and reduced standby power consumption.**

***Index Terms*— Energy efficiency, light-emitting diode (LED), lighting control, switched-mode power supply.**

I. Introduction

THE light-emitting diode (LED) is an emerging light source due to its high luminous efficacy (lumen per watt) and longevity. The benefits of LED lighting include a theoretical efficacy capability of over 200 lm/W and a long lifetime, up to 100 000 h, attributed to advances in solid-state lighting technology [1]–[4]. Owing to these advantages, LED lamps have been employed in a variety of applications, such as liquid crystal display backlights for displays [5], automobiles [6], and general purpose lightings for indoor and outdoor use [7]. In particular, LED lighting for indoor use is one of the most promising application areas, because a significant amount of energy is consumed by building lighting [8]–[10]. In addition, the long lifetime of LED lamps is beneficial for building lighting systems because they require less maintenance.

While the lifetime of LED lamps is relatively long, the lifespan of the lamp driving circuit is shorter, which is a major constraint to wide application of LED lighting. Because the lifetime of the LED system is currently limited by the driver circuit, extending the lifetime of the driver to match that of the lamp is crucial to enabling LED lighting as a viable option [2], [11]. The main limiting factor of the driving circuit's lifespan is its electrolytic capacitors. The lifetime for electrolytic capacitors is only up to 10 000 h at specified operating conditions, which is only about a tenth of the LED lamp lifetime [12]. Electrolytic capacitors are commonly used to decoupling the dc-driven LED from the ac side because they provide high energy density and cost-effectiveness. Thus, the main challenge is to maintain proper performance while extending the driver's lifespan closer to that of the LED lamp.

To avoid the use of the lifetime-limiting capacitors in the LED driver circuit, several approaches have been presented. In [2] and [12], the voltage ripple at the dc link capacitor is intentionally increased with modified driving current and harmonic injection techniques, respectively, to reduce its reliance on the bulky energy buffer. As a result, the reduced requirement of decoupling capacitance allows electrolytic capacitor-less drivers. These methods extend the expected lifetime of the circuits using long-lifetime film capacitors employed instead of electrolytic ones. However, they also increase circuit complexity and require high-performance control processors.

Another attractive solution that overcomes the short lifetime of the LED driver is to completely change the building distribution system to dc rather than the traditional ac [13]–[15]. In the conventional ac distribution system, LED drivers must include an ac–dc power factor correction circuit that has an electrolytic capacitor energy buffer in order to meet industry standards for the regulated power factor and total harmonic distortion, such as the IEC-61000-3-2 standard [16], [17]. As a result, this conventional ac distribution practice inevitably encounters driver lifetime issues caused by the bulky decoupling electrolytic capacitors. Alternatively, dc distribution intrinsically reduces the need for the electrolytic capacitors. Because the front-end ac–dc converter decoupling is not needed in dc distribution systems, film capacitors can directly replace electrolytic ones without the need for sophisticated methods [18], [19]. In short, a dc LED lighting distribution system would naturally alleviate the lifetime issue of the LED drivers, because the

Manuscript received November 16, 2014; revised January 16, 2015, February 16, 2015, and March 19, 2015; accepted March 21, 2015. Date of publication March 25, 2015; date of current version July 30, 2015. This work was supported by the Human Resources Development program (No. 20124030200030) of the Korea Institute of Energy Technology Evaluation and Planning (KETEP) grant funded by the Korea government Ministry of Trade, Industry and Energy. Recommended for publication by Associate Editor Georges Zissis.

G.-S. Seo, H.-J. Kim, and B.-H. Cho are with the Department of Electrical and Computer Engineering, Seoul National University, Seoul 151-742, Korea (e-mail: gabzzu@snu.ac.kr; gpwls12@snu.ac.kr; bhcho@snu.ac.kr).

K.-C. Lee is with Smart Power Supply, Ltd., Seoul 137-838, Korea (e-mail: kyuchan6@empas.com).

S.-J. Choi is with the School of Electrical Engineering, University of Ulsan, Ulsan 680-749, Korea (e-mail: sjchoi@ulsan.ac.kr).

Color versions of one or more of the figures in this paper are available online at http://ieeexplore.ieee.org.

Digital Object Identifier 10.1109/JESTPE.2015.2416979

lifetime-limiting electrolytic capacitors would be eliminated. As renewable sources, such as dc-generating photovoltaics, are more widely used and are substituted for conventional power sources, and as more electric appliances utilize dc power input, such as solid-state lightings and inverter-driven devices, adopting dc distribution in buildings will become more common practice, as it is more effective for interfacing dc-based sources and loads [20], [21].

This paper discusses a new LED light dimming scheme, preliminarily presented in [22], that assumes dc distribution has been adopted in the target building. Compared with [22], this paper provides more detailed analyses, discussion, and design guidelines for implementation in the target systems of offices or parking lots. This paper details operation principles of the proposed dimming scheme and design guidelines for the practical implementation of a dc-level dimmable LED driving circuit. It also provides extended experimental results and discussions. The proposed LED light dimming scheme is referred to as dc-level dimming in this paper. It utilizes a simple architecture with minimum communication interfaces to achieve improved system efficiency from higher driver efficiency and lower standby power consumption compared with the conventional one, which uses additional communication modules and wires for dimming.

This paper is organized as follows. The schematic of the proposed lighting system and its key advantages are discussed in Section II. Section III presents the operation principle and design considerations for the LED driver circuit. A prototype circuit design and its experimental results verify the feasibility of the circuit in Section IV. The performance of the proposed method in the target system is analyzed in Section V. Finally, the conclusion is drawn in Section VI.

II. DC-Level Dimmable LED Lighting System

The proposed dimming method enhances a dimmable LED lighting system in terms of system configuration and system efficiency. First, for the system configuration, the method utilizes a simple architecture that provides advantages in dimming, ballast power density, installation, and maintenance. To confirm the advantages of the proposed method, the operation principles of it and its conventional counterpart are examined. Fig. 1 compares two dc LED systems: 1) with the dc-level dimming, shown in Fig. 1(a) and 2) with conventional dimming, shown in Fig. 1(b), using communication. The proposed dimmable LED lighting system, in Fig. 1(a), includes dc-level dimmers and LED drivers. As shown in Fig. 2, this dc-level dimming scheme has three operation modes: 1) nondimming; 2) dimming; and 3) shutdown. It operates in the nondimming mode above $v_{\mathrm{dim\_ST}}$, in the dimming mode from $v_{\mathrm{dim\_ST}}$ to $v_{\mathrm{dim\_SD}}$, and in shutdown mode below $v_{\mathrm{dim\_SD}}$. The dc-level dimmer #n in zone #n sets its output voltage v_{dim_n} according to the dimming signal, as described in Fig. 1(a). The following drivers in the same zone adjust their LED brightness depending on the level of v_{dim_n}; therefore, the brightness of the LED lamps in the zone is controlled at the same level. It is common practice to control a group of lights that are placed in an equally lit area or designed to have the same brightness, such as LED drivers, in the same zone [23].

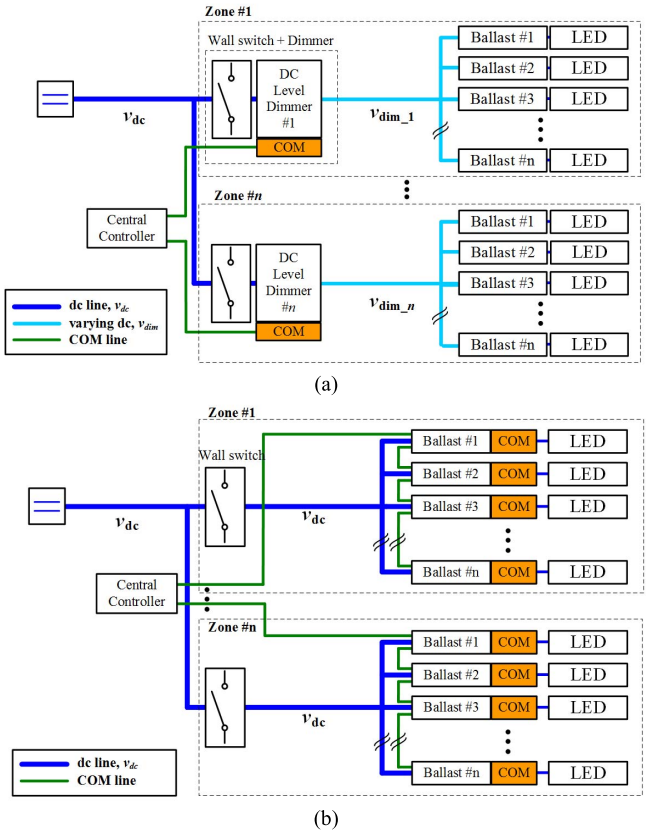

Fig. 1. Comparison of dc LED lighting systems. (a) Proposed dc-level dimming. (b) Conventional one with individual communication modules.

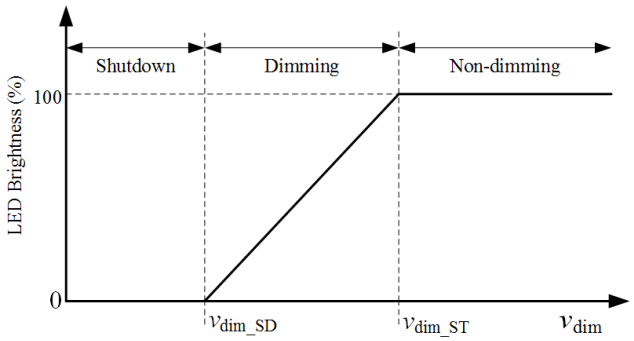

Fig. 2. Operation principle of the dc-level dimming scheme.

Since this dc-level dimming requires no communication lines between dimmer and drivers, its architecture is simple and driver size is reduced, since communication modules are not needed. In addition, the proposed method reduces system maintenance and makes retrofitting nondimmable lighting system easier because there are no additional wires needed for dimming [24].

In the conventional system, each driver circuit should receive a dimming signal from the controller using its own communication module, as shown in Fig. 1(b). In practice, the zoning method used in Fig. 1(a) would be applied for the same purpose. As a result, the conventional practice requires additional wires for carrying the dimming signal. This dual wire configuration significantly increases system complexity and, thus, causes difficulties with maintenance and retrofitting. In summary, the proposed dc-level dimming

scheme has a simpler architecture with dimming functionality, reduced ballast size, and advantages in maintenance and retrofitting compared with the conventional system.

Second, in addition to the benefits from the simple architecture, the proposed method achieves improved efficiency through increased light-load efficiency by the varying ballast input voltage. The total efficiency of the system with multiple power stages, between the source and the load, is improved by adopting a variable bus voltage. This concept has been widely studied and its feasibility has been verified [25], [26]. In the same manner, the LED lighting system efficiency can be improved by properly matching $v_{\rm dim}$ to the level of the LED brightness. In this paper, the claim on the system efficiency improvement is confirmed by loss analysis of a critical conduction mode (CRM) flyback type LED driver. The CRM flyback circuit is widely used for the LED application in tens of watt range due to the simplicity of the power circuit and high efficiency achieved by soft switching [27]. Although the following analysis presents a specific topology and operating mode, the method can also be applied to a variety of configurations. In the analysis, switching loss is examined first because it is the dominant loss at light load condition and, thus, heavily affects the light load efficiency. Conduction loss analysis is conducted later to derive the total loss and driver efficiency.

In CRM operation, the MOSFET switching loss, which can be divided into the turn ON and OFF loss, is expressed as

$$P_{\rm loss\_SW\_on} = 0.5 \cdot C_{\rm ds} \cdot (v_{\rm dim} - n \cdot v_o)^2 \cdot f_s \qquad (1)$$

and

$$P_{\rm loss\_SW\_off} = 0.5 \cdot T_{\rm fall} \cdot (v_{\rm dim} + n \cdot v_o) \cdot i_{L\_\rm pk} \cdot f_s \qquad (2)$$

respectively [28]. In (1) and (2), $C_{\rm ds}$, n, v_o, f_s, $T_{\rm fall}$, and $i_{L\_\rm pk}$ are the effective drain–source capacitance, flyback transformer turns ratio from the secondary to primary side, converter output voltage, switching frequency, falling time of the MOSFET switch, and peak current of the magnetizing inductor on the transformer primary side, respectively. In this analysis, diode reverse recovery loss, the major diode switching loss, is assumed to be negligible due to CRM operation [29]. The current and voltage waveforms are assumed to be linear, which enables the approximations of (1) and (2). The chance to improve the efficiency by the proposed dimming scheme is assured both in (1) and (2) as the loss increase in light load would be suppressed by decreasing $v_{\rm dim}$. Conversely, in a conventional CRM converter operating with constant input voltage, the switching losses drastically increase in the same condition due to the frequency increase.

To confirm the resultant efficiency improvement of the dc-level dimming scheme, the conduction loss figures are also derived. For the conduction losses, the summation of MOSFET, diode, and magnetic copper conduction losses is derived as

$$P_{\rm loss\_cond} = R_{\rm ds\_on} \cdot i_{\rm sw\_rms}^2 + v_f \cdot i_d + R_L \cdot i_{L\_\rm rms}^2 \qquad (3)$$

where $R_{\rm ds\_on}$, $i_{\rm sw\_rms}$, v_f, i_d, R_L, and $i_{L\_\rm rms}$ are the ON resistance and rms current of MOSFET, diode forward voltage, average diode current, equivalent transformer winding resistance, and rms inductor current, respectively. According to (3), it is inferred that the conduction loss of the proposed method would be relatively large as the current figures, $i_{\rm sw\_rms}$ and $i_{L\_\rm rms}$, increase when the input voltage is decreased.

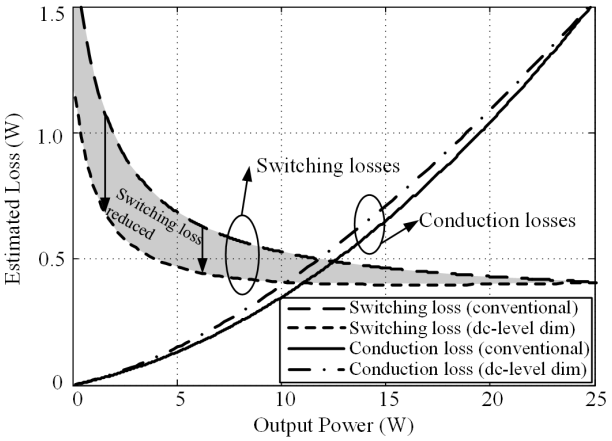

Fig. 3. Estimation of loss factors in the dc-level dimming and conventional system.

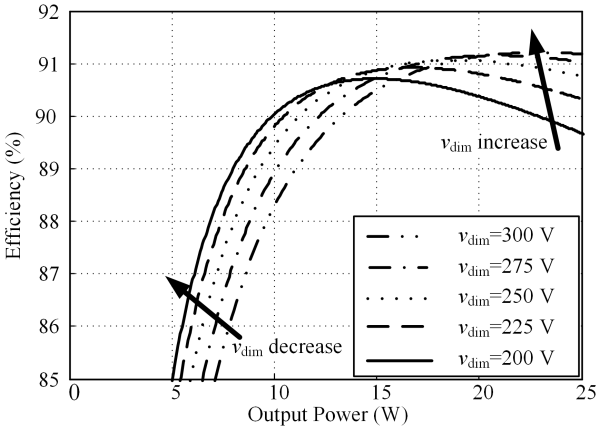

Fig. 4. Efficiency estimation with $v_{\rm dim}$ as a running parameter.

Based on the loss factor derivations, a graphical approach is presented for practical analysis. In this analysis, the dc-level dimming system is assumed to allocate 200 V for $v_{\rm dim\_SD}$ and 300 V for $v_{\rm dim\_ST}$. The conventional system is assumed to use 300 V for the individual drivers in this comparative analysis. The analysis results, displayed in Fig. 3, clearly verify the benefits of the proposed scheme, showing that the variable intermediate voltage effectively suppresses the switching losses. The difference between the conduction losses is not significant, such that it has little influence on the efficiency difference over the full operating range. This result is understood by noting that the rms currents, $i_{\rm sw\_rms}$ and $i_{L\_\rm rms}$, in (3), decrease in square manner as the load decreases in both cases.

In addition to the loss analysis, the efficiency estimations in Fig. 4 show the dependence of the driver efficiency on $v_{\rm dim}$ and the achievable efficiency improvement using variable input voltages for different load conditions. In conclusion, the new scheme cannot only be used for dimming but also be used to match a specific load condition for system efficiency improvement.

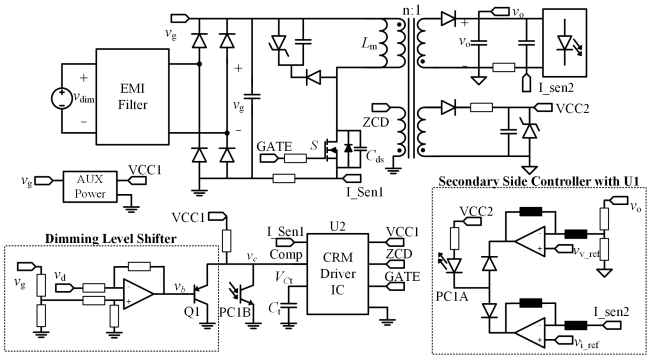

Fig. 5. DC-level dimmable LED driver with proposed dimming level shifter.

III. Design of DC-Level Dimmable Ballast

To realize the proposed lighting system, a detailed design guideline for the dc-level dimmable driver is presented. The main function of this driver circuit is to properly interpret the level of its input voltage into an LED current control signal. This circuit is called a dimming level shifter in this paper. A variety of dimming level shifter circuits can be realized utilizing analog and/or digital techniques, depending on the system requirements, such as accuracy and cost. If the system requires high current regulation accuracy, the cost increases. On the other hand, cost can be reduced if high accuracy is not required. Assuming the system requires low cost, a dimming level shifter with compact circuitry is proposed in this paper as a feasible solution. It can be implemented only with one differential operational amplifier with resistors to measure the input voltage information and one signal transistor to modify the control signal in dimming mode. Fig. 5 shows its circuit diagram, and the operation principle and design guide for this implementation are presented.

A. Operation Principle

The dc-level dimmable flyback converter, shown in Fig. 5, is regulated by the secondary side controller in the nondimming condition, similar to a battery charger [30]. The form of diode-OR at the output of the error amplifiers enables the LED current regulation in normal operation due to the saturation of the voltage loop as the voltage reference is set slightly higher than the rated voltage of the LED lamp. The voltage loop takes effect in a fault or no load condition, suppressing the output voltage overshoot. The controller U1 on the secondary side in Fig. 5 uses an optocoupler to modulate the gate signal for the switch S in the primary side for isolation. U2 on the primary side directly drives the MOSFET switch according to the control signal and achieves CRM operation using a zero current detection circuit.

In addition to the secondary side-induced control, a primary side-induced dimming level shifter is dispatched for the proposed dimming operation. This dimming level shifter, highlighted in Fig. 5, consists of a differential amplifier to obtain the level of the input voltage and, resultantly, to set v_b, which modulates the control voltage v_c in the dimming condition, as described in Fig. 6. The voltage v_d in the dimming level shifter is a regulated voltage reference to be

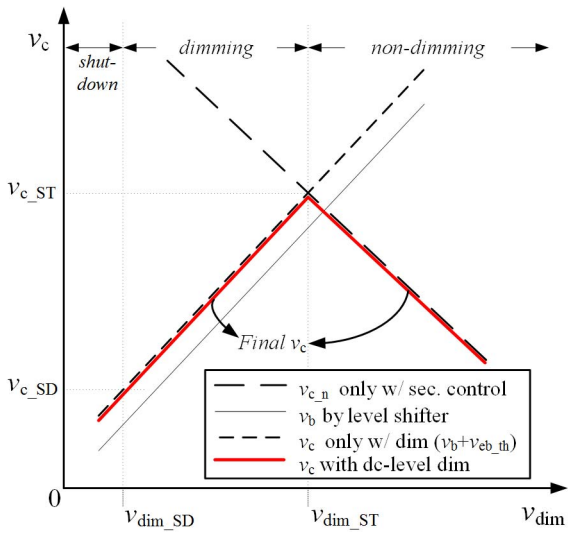

Fig. 6. Operation principle of the dimming level shifter.

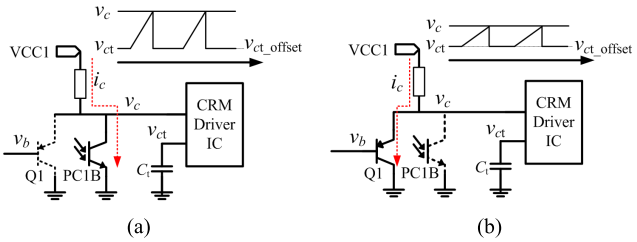

Fig. 7. Equivalent circuits of the on-time modulation circuit in (a) nondimming operation and (b) dimming operation.

compared with the input voltage for dimming operation. In the nondimming condition, where the input voltage is kept higher than $v_{\text{dim\_ST}}$, v_b is kept high in order to satisfy

$$v_{c\_n} - v_b < v_{\text{eb\_th}} \tag{4}$$

where v_{c_n} and $v_{\text{eb\_th}}$ are the control voltage set by the secondary side current controller without the dimming level shifter and threshold emitter–base voltage to turn ON Q1. Therefore, in the nondimming operation, the dimming level shifter exerts no influence on the current control with Q1 turned OFF, as shown in Fig. 7(a).

On the other hand, in the dimming condition where the input voltage is lower than $v_{\text{dim\_ST}}$, (4) is no longer satisfied; the base voltage v_b drops low enough to turn ON Q1, which causes the control voltage v_c to be solely determined by the dimming level shifter, as shown in Fig. 7(b). Once v_{dim} drops under $v_{\text{dim\_ST}}$, the secondary side current controller does not influence the control voltage modulation as it saturates to the upper bound, which causes no current through optocoupler PC1. As a result, the control voltage v_c is shaped, as shown in Fig. 6, and the proposed dimming method is realized by the dimming level shifter.

The proposed method still guarantees the same protection capabilities as the conventional solutions. The secondary side device protections, such as over current and voltage protection, are available regardless of operation modes. In addition, the bridge rectifier following the electromagnetic interference (EMI) filter in Fig. 5 provides the reverse bias voltage protection at the input; however, it causes

additional conduction losses that reduce the driver efficiency. For instance, 0.37% of the total processing power dissipates in the bridge rectifier, assuming a 380 V input and 0.7 V constant diode drop (a 1.4 V drop in total).

In conclusion, this proposed primary side dimming control enables the direct modification of the control signal with no additional signal isolation and without compromised protection.

B. Design Considerations

Since the dc-level dimming method is utilized to improve the system efficiency, the decision process of the operation voltage range should be conducted based on the loss analysis presented in Section II. After the operating conditions are recognized, the driver circuit parameters related to both power processing and LED control can be designed referring to the conventional converter design method [27]. Therefore, this paper only details the parameter design for the dimming level shifter.

In designing the dimming level shifter, the starting and shutdown input voltages, $v_{\text{dim\_ST}}$ and $v_{\text{dim\_SD}}$, and the corresponding desired control voltages, v_{c_ST} and v_{c_SD}, are identified by considering the operating principle and specifications of the commercial ICs used in the circuit. As described in Fig. 6, v_{c_ST} is designed to equal the sum of the base voltage of Q1, v_b, and emitter–base voltage at $v_{\text{dim\_ST}}$, $v_{\text{eb\_ST}}$, to turn ON Q1 to start the dimming operation at $v_{\text{dim\_ST}}$, expressed as

$$k_d \cdot (k_v \cdot v_{\text{dim\_ST}} - v_d) + v_{\text{eb\_ST}} = v_{c\_\text{ST}} \tag{5}$$

where k_d and k_v are the gain of the differential amplifier and the input voltage divider, respectively. Furthermore, v_{c_SD} should be equal to $v_b + v_{\text{eb\_SD}}$ to shutdown the ballast at $v_{\text{dim\_SD}}$, expressed as

$$k_d \cdot (k_v \cdot v_{\text{dim\_SD}} - v_d) + v_{\text{eb\_SD}} = v_{\text{c\_SD}}. \tag{6}$$

Assuming the constant emitter–base voltage in (5) and (6) and subtracting (6) from (5) yields

$$k_d \cdot k_v \cdot (v_{\text{dim\_ST}} - v_{\text{dim\_SD}}) = v_{c\_\text{ST}} - v_{c\_\text{SD}} \tag{7}$$

which indicates that the circuit can be implemented by properly designing the gain factors k_d and k_v for the specified operation.

As the proposed primary side on-time control is an indirect control method, the current regulation characteristics depend on the circuit parameters and operation [31], [32]. Considering the circuit parameters and CRM operation to estimate the current regulation, the LED current can be derived as

$$I_o = \frac{0.5 \cdot \frac{v_{\text{dim}}^2 T_{\text{ON}}^2}{L_m \cdot v_o}}{\left(1 + \frac{v_{\text{dim}}}{n \cdot v_o}\right) \cdot T_{\text{ON}} + T_r + T_{\text{rise}}} \tag{8}$$

where T_{ON}, T_r, and T_{rise} are the on-time of the main switch, the duration of the resonance between L_m and C_{ds}, and the time for fully charging up the junction capacitor to $v_{\text{dim}} + n \cdot v_o$ with the constant magnetizing current assumption during ON-to-OFF state [32]. In (8), nonlinearity between v_{dim} and I_o is expected, which can be considered in the design process to match the input voltage to the desired level of dimming. The feasibility of the derivation is discussed in Section IV with experimental results.

The primary side on-time regulation method for the dc-level dimming control features little additional part counts for implementation and, accordingly, little additional power consumption. Design considerations related to the system realization are presented in Section IV with a prototype circuit implementation.

IV. Implementation and Experimental Results

To verify the feasibility of the proposed method, a prototype LED driver for a 24-W LED lamp, whose rated operating condition is 48 V/0.5 A, is realized; 75 LEDs are connected in series per an LED lamp. The operating conditions and main circuit parameters are specified as follows.

1) $v_{\text{dim\_max}}$: 380 V; $v_{\text{dim\_ST}}$: 300 V; $v_{\text{dim\_SD}}$: 200 V.
2) Transformer: EE1011 Core; $n:1 = 100{:}27$.
3) L_m: 3 mH.
4) MOSFET: STF3NK80Z.
5) Diode: MBRS3201T3.
6) Voltage/current controller (U1): TMS101.
7) CRM driver (U2): NCL30000; $v_{\text{ct\_offset}}$: 0.65 V; C_t: 0.9 nF.
8) Q1: 2N3906.
9) f_s: 55–120 KHz depending on v_{dim} and the dimming condition.

A 2-poles-2-zeros (2P2Z) feedback loop for the current regulation and proportional-integral (PI) voltage loop are implemented.

In addition to the predetermined circuit parameters for the rated operation, parameters for dimming operation are designed. First, the parameters in (7) are determined considering the electrical characteristics of the CRM control IC and its control circuit configuration. For shutdown operation, a practical method is to utilize the internal comparator offset of the CRM control ICs, which is usually used for noise immunity, as shown in Fig. 7. In this implementation, the shutdown function is realized by positioning v_{c_SD} at the offset voltage $v_{\text{ct\_offset}}$. v_{c_ST} is determined by the relationship of the on-time capacitor C_t, internal on-time capacitor charging current i_{ct}, and turn ON time $T_{\text{on\_ST}}$ at $v_{\text{dim\_ST}}$, which is expressed as

$$v_{c\_\text{ST}} = \frac{1}{C_t} T_{\text{on\_ST}} \cdot i_{\text{ct}} + v_{\text{ct\_offset}}. \tag{9}$$

$T_{\text{on\_ST}}$ can be calculated considering the circuit parameters. After the control voltages are determined, the voltage divider gains are designed to satisfy (7) as follows.

10) k_d: 1.
11) k_v: 0.013.

The design parameter v_d is determined to satisfy (5) and (6) with a specified $v_{\text{eb\_ST}}$ or $v_{\text{eb\_SD}}$. The reference voltage v_d is determined as 2.5 V by the constant emitter–base voltage assumption, which would cause some difference in the control voltages between the design and the implementation. Thus, it could result in controlled current variations, which is discussed with the experimental results.

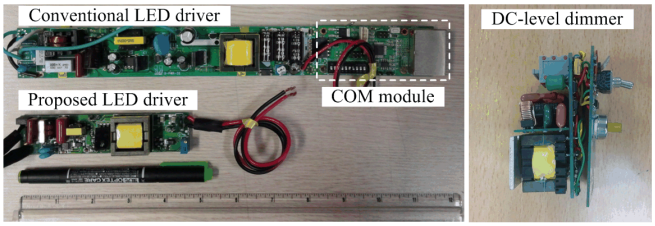

Fig. 8. Conventional and proposed dimmable LED driver, and dc-level dimmer.

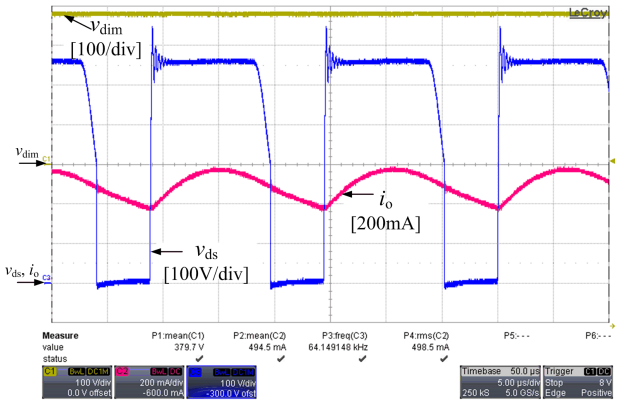

Fig. 9. Experimental waveforms at 380 v_{dim} condition with switch voltage.

For comparison, the conventional circuit is also realized and operates with a constant input voltage of 380 V dc. To operate in the dc environment, a commercial dimmable product is modified. The topology of the counterpart is the same with the proposed circuit, CRM flyback, and the transformer's turn ratio is modified to be equal to that of the prototype, 100:27, to increase its efficiency at the 380 V input condition. In addition, the surge suppressor rated at 400 V input replaces the previous ac universal input. Each conventional LED driver is equipped with a communication module for the dimming operation, as shown in Fig. 1(b).

The prototype circuit is implemented according to the design procedure, and realization and experimental results are discussed for verification. Fig. 8 shows the photographs of the dc-level dimmer and the two dimmable LED circuits: 1) the conventional LED driver using the communication module for dimming and 2) the proposed dc-level dimmable driver. Experimental results of the prototype are presented in Figs. 9–12 with the operation waveforms, which are in agreement with the discussion in Section III. In Fig. 9, the driver regulates the LED current at the rated value with the control voltage set by the secondary side, which confirms the nondimming operation at 380 V input. The CRM operation is also proved in Fig. 9. Fig. 10 verifies the nondimming operation at the same condition with additional waveforms. It shows the operation waveforms of the control voltage v_c and base voltage v_b. Since v_b is far above v_c, it is clear that the secondary side controller has the authority of control, as shown in Fig. 7(a).

Fig. 11 shows 340 V v_{dim} operation; the converter still operates in the nondimming condition as designed with Q1 under cutoff mode. Fig. 12 shows the operation at 250 V v_{dim}, where the primary dimming level shifter

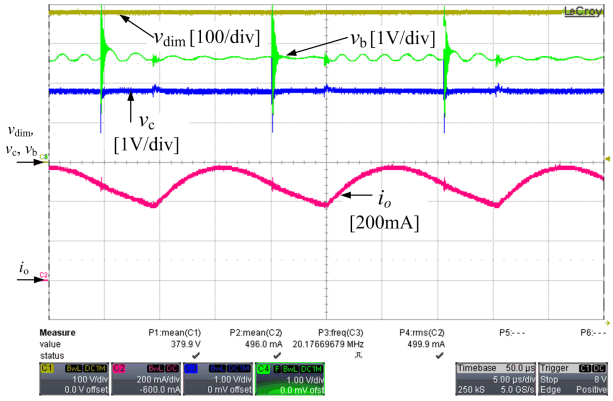

Fig. 10. Experimental waveforms at 380 v_{dim} condition with control voltages.

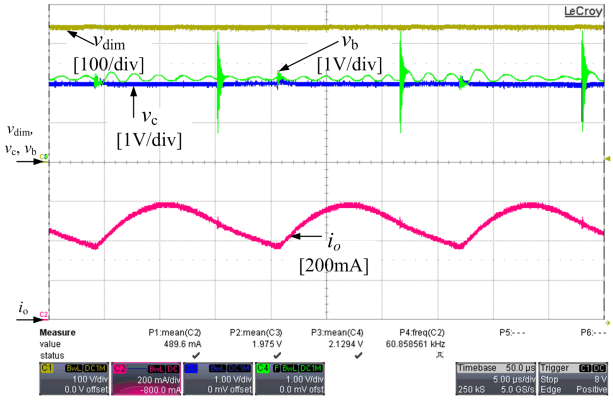

Fig. 11. Experimental waveforms at 340 v_{dim} condition.

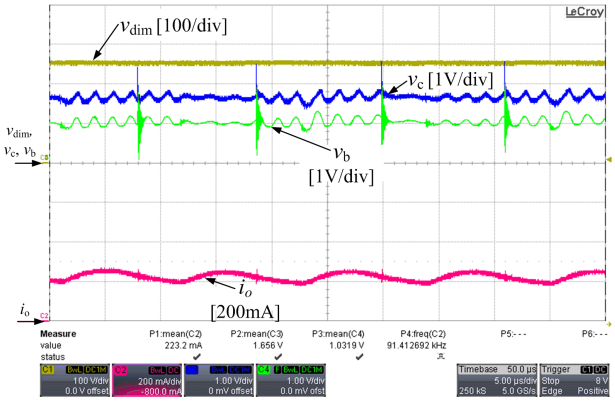

Fig. 12. Experimental waveforms at 250 v_{dim} condition.

solely conducts the on-time control with the secondary side controllers saturated, as shown in Fig. 7(b). It also shows that the operating frequency is well suppressed under 100 kHz, unlike the conventional CRM converters, attributed to the decreased driver input voltage, as analyzed in Section II.

Fig. 13 details the estimated LED current from (8) and the measured at different input voltages. As the results show, the nonlinearity between the voltage and the current is observed in the experiment, which was previously analyzed in Section III. In addition, the difference between the estimation and the measurement is caused by not knowing the exact forward voltage of the LED lamp, which tends to slightly decrease

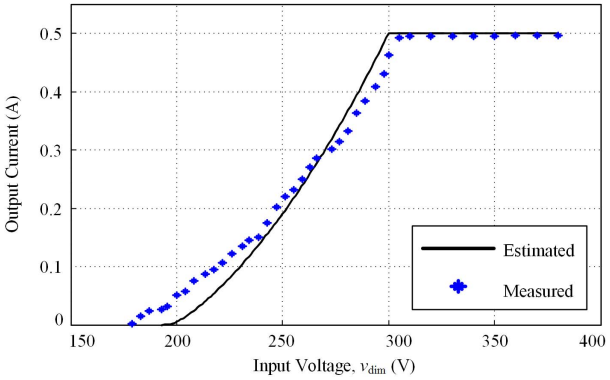

Fig. 13. Estimated and measured dimming current regulation.

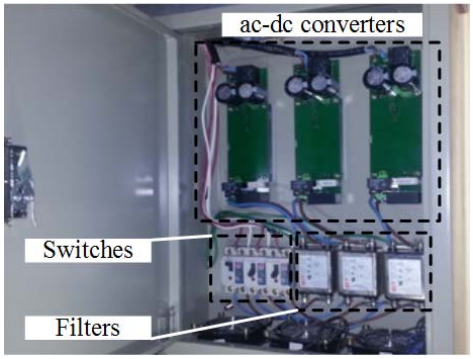

Fig. 14. DC distribution unit for parking lot LED system.

as its current decreases and the assumption of constant magnetizing inductor current of flyback transformer during the ON-to-OFF transient charging up C_{ds} for the analysis simplicity. In addition, the electrical characteristic of Q1 would also be one of the causes, since it is assumed to have the constant emitter–base voltage even with the varying collector current in the analysis as addressed in the design guide.

V. System Realization

Following the discussion of the prototype LED driver circuit, the system realization results of the dc LED lighting system are examined. This paper targets a two-story parking lot in which 380 V dc lines are distributed to verify the dimming technology. As the dc power is not yet directly supplied by the electric power corporation in the site, distribution units for supplying 380 V dc power to the building are employed. In the target area, ninety 24-W LED lamps are operated by the dc-level dimming scheme on one floor, while the other ninety 24-W LED lamps are controlled by the conventional dimming on the other floor. Fig. 14 shows the distribution unit, which accommodates circuit breakers, EMI filters, and ac–dc converters. A 150-W buck converter regulates v_{dim} ranging from 200 to 300 V, according to the dimming signal for six flyback LED drivers in a group. The pass-through mode, which makes the 380 V dc link voltage directly appear at the input of the following drivers, is employed to improve the system efficiency in the nondimming operation. In addition, in the shutdown mode, the dimmer disables its output, which dramatically reduces the standby power consumption. After the dimmer, the prototype LED driving circuits drive the 24-W LED lamps, as designed

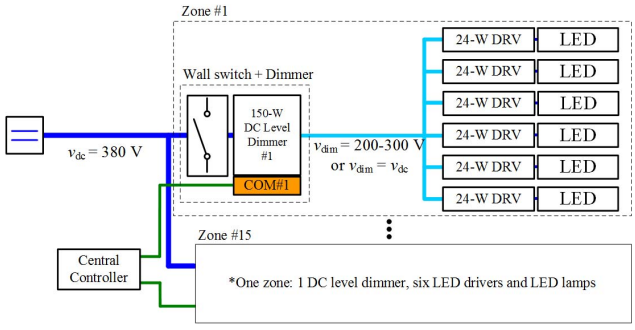

Fig. 15. DC-level dimming LED system configuration for target parking lot.

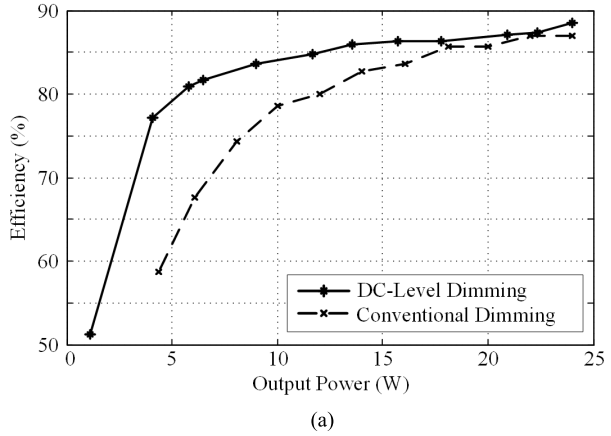

(a)

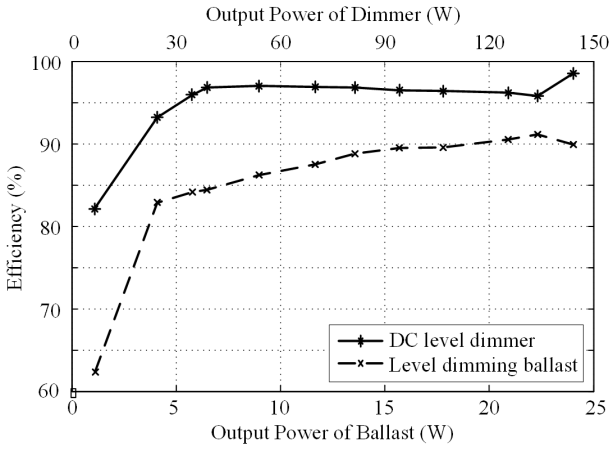

(b)

Fig. 16. Measured efficiency comparison. (a) Efficiencies of proposed and conventional system. (b) Efficiencies of dc-level dimmer and dc-level dimmable ballast.

in Section IV. Fig. 15 details the configuration of the proposed dc-level dimming LED system implementation for the target parking lot.

Finally, the efficiency figures of the dc LED lighting systems are discussed in detail. Fig. 16(a) compares the measured system efficiencies of the proposed lighting system to the conventional one at different loads. The efficiency of the dc-level dimmer in the new system is included for the total efficiency comparison. In addition, Fig. 16(b) details the efficiency figures of the dc-level dimmer and proposed LED driver. To provide the insight into the total efficiency at individual load conditions, x-axis of the dimmer efficiency data is six times that of the ballasts, as one dc-level dimmer

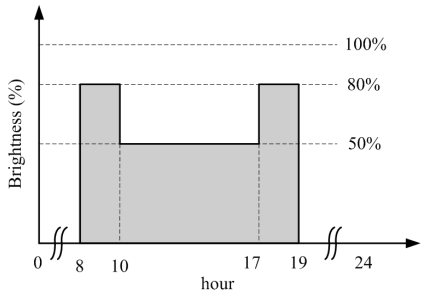

Fig. 17. Dimming profile for energy saving derivation.

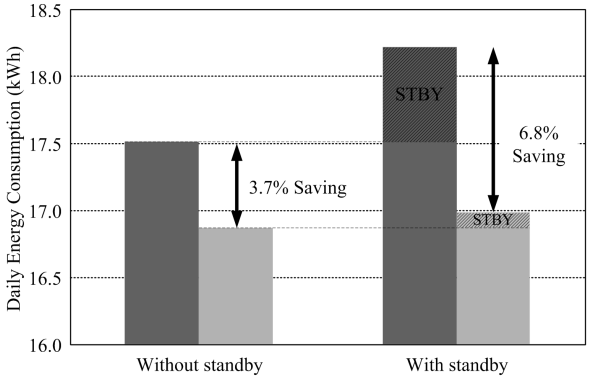

Fig. 18. Energy saving figures considering standby power consumption.

operates six ballasts. The measured data agree with and verify the analysis in Section II; they clearly show the efficiency improvement of the proposed method in dimming conditions. In addition, the standby power is also measured to estimate the total daily energy saving. Each auxiliary power supply for the controller and communication module used in the experiment consumes ∼0.6 W in standby operation. In this analysis, it is assumed that the two systems operate under the same LED dimming and standby operation according to the profile displayed in Fig. 17. As one dimmer accommodates six LED lamps in each zone, it allows the proposed system to consume 83.3% less standby power; each conventional driver would consume the standby power itself. Based on the measurements, this analysis concludes 6.8% total energy saving by the dc-level dimming compared with the conventional one; 3.7% and 3.1% are achieved by the improved efficiency of the new driving circuit and reduced standby power consumption, respectively, as detailed in Fig. 18. The energy saving figures are derived from the two energy consumption data expressed as

$$\eta_{\text{saving}}(\%) = (E_{\text{conv}} - E_{\text{prop}})/E_{\text{conv}} \tag{10}$$

where E_{conv} and E_{prop} are the daily energy consumptions of the conventional and proposed systems, respectively.

VI. Conclusion

In this paper, a dc LED lighting system using a dc-level dimming technique has been proposed. The dimmable lighting system features a simple architecture and improved efficiency as the main benefits compared with the conventional dc-powered LED lighting system, which uses communication modules and additional wires for dimming. The proposed system realizes dimming control with minimum communication interfaces, such that it achieves ease of installation, maintenance, and retrofitting. By varying input voltage to match the LED loads, it also achieves improved light load efficiency as well as lower standby power consumption compared with the conventional system. The dimming level shifter with a differential operational amplifier for the primary side on-time regulation enables the LED driver to control the LED brightness according to the input voltage, while its operation principle, using a parallel bipolar transistor, still permits the conventional overcurrent and voltage protection. The design considerations for the system implementation have presented the design equations, and the experimental results of the prototype LED driver verified the feasibility of the proposed dimming method. The dc-level dimming and conventional LED lighting system for the target parking lot application with two sets of ninety LED lamps have been realized to validate the system feasibility. The power consumption measurements verify 6.8% energy saving through the higher conversion efficiency and reduced standby power consumption by 3.7% and 3.1%, respectively.

References

[1] C. Branas, F. J. Azcondo, and J. M. Alonso, "Solid-state lighting: A system review," *IEEE Ind. Electron. Mag.*, vol. 7, no. 4, pp. 6–14, Dec. 2013.

[2] F. Zhang, J. Ni, and Y. Yu, "High power factor AC–DC LED driver with film capacitors," *IEEE Trans. Power Electron.*, vol. 28, no. 10, pp. 4831–4840, Oct. 2013.

[3] M. G. Craford, "From Holonyak to today," *Proc. IEEE*, vol. 101, no. 10, pp. 2170–2175, Oct. 2013.

[4] X. Qu, W. Zhang, S.-C. Wong, and C. K. Tse, "Design of a current-source-output inductive power transfer LED lighting system," *IEEE J. Emerg. Sel. Topics Power Electron.*, vol. 3, no. 1, pp. 306–314, Mar. 2015.

[5] S. Choi and T. Kim, "Symmetric current-balancing circuit for LED backlight with dimming," *IEEE Trans. Ind. Electron.*, vol. 59, no. 4, pp. 1698–1707, Apr. 2012.

[6] S. Saponara, G. Pasetti, N. Costantino, F. Tinfena, P. D'Abramo, and L. Fanucci, "A flexible LED driver for automotive lighting applications: IC design and experimental characterization," *IEEE Trans. Power Electron.*, vol. 27, no. 3, pp. 1071–1075, Mar. 2012.

[7] D. Camponogara, G. F. Ferreira, A. Campos, M. A. D. Costa, and J. Garcia, "Offline LED driver for street lighting with an optimized cascade structure," *IEEE Trans. Ind. Appl.*, vol. 49, no. 6, pp. 2437–2443, Nov./Dec. 2013.

[8] D. Tran and Y. K. Tan, "Sensorless illumination control of a networked LED-lighting system using feedforward neural network," *IEEE Trans. Ind. Electron.*, vol. 61, no. 4, pp. 2113–2121, Apr. 2014.

[9] W. A. Rodrigues, L. M. F. Morais, P. F. Donoso-Garcia, P. C. Cortizo, and S. I. Seleme, "Comparative analysis of power LEDs dimming methods," in *Proc. 37th Annu. Conf. IEEE Ind. Electron. Soc.*, Nov. 2011, pp. 2907–2912.

[10] D. Boroyevich, I. Cvetkovic, R. Burgos, and D. Dong, "Intergrid: A future electronic energy network?" *IEEE J. Emerg. Sel. Topics Power Electron.*, vol. 1, no. 3, pp. 127–138, Sep. 2013.

[11] D. G. Lamar, M. Arias, A. Rodriguez, A. Fernandez, M. M. Hernando, and J. Sebastian, "Design-oriented analysis and performance evaluation of a low-cost high-brightness LED driver based on flyback power factor corrector," *IEEE Trans. Ind. Electron.*, vol. 60, no. 7, pp. 2614–2626, Jul. 2013.

[12] L. Gu, X. Ruan, M. Xu, and K. Yao, "Means of eliminating electrolytic capacitor in AC/DC power supplies for LED lightings," *IEEE Trans. Power Electron.*, vol. 24, no. 5, pp. 1399–1408, May 2009.

[13] B. A. Thomas, "Edison revisited: Impact of DC distribution on the cost of LED lighting and distributed generation," in *Proc. 25th IEEE Appl. Power Electron. Conf. Expo.*, Feb. 2010, pp. 588–593.

[14] Y. K. Tan, T. P. Huynh, and Z. Wang, "Smart personal sensor network control for energy saving in DC grid powered LED lighting system," *IEEE Trans. Smart Grid*, vol. 4, no. 2, pp. 669–676, Jun. 2013.

[15] O. Lucia, I. Cvetkovic, H. Sarnago, D. Boroyevich, P. Mattavelli, and F. C. Lee, "Design of home appliances for a DC-based nanogrid system: An induction range study case," *IEEE J. Emerg. Sel. Topics Power Electron.*, vol. 1, no. 4, pp. 315–326, Dec. 2013.
[16] Y. Hu, L. Huber, and M. M. Jovanovic, "Single-stage, universal-input AC/DC LED driver with current-controlled variable PFC boost inductor," *IEEE Trans. Power Electron.*, vol. 27, no. 3, pp. 1579–1588, Mar. 2012.
[17] Y.-C. Li and C.-L. Chen, "A novel primary-side regulation scheme for single-stage high-power-factor AC–DC LED driving circuit," *IEEE Trans. Ind. Electron.*, vol. 60, no. 11, pp. 4978–4986, Nov. 2013.
[18] D. Dong, I. Cvetkovic, D. Boroyevich, W. Zhang, R. Wang, and P. Mattavelli, "Grid-interface bidirectional converter for residential DC distribution systems—Part one: High-density two-stage topology," *IEEE Trans. Power Electron.*, vol. 28, no. 4, pp. 1655–1666, Apr. 2013.
[19] G.-S. Seo, K.-C. Lee, and B.-H. Cho, "A new DC anti-islanding technique of electrolytic capacitor-less photovoltaic interface in DC distribution systems," *IEEE Trans. Power Electron.*, vol. 28, no. 4, pp. 1632–1641, Apr. 2013.
[20] V. Vossos, K. Garbesi, and H. Shen, "Energy savings from direct-DC in U.S. residential buildings," *Energy Buildings*, vol. 68, pp. 223–231, Jan. 2014.
[21] J. D. van Wyk and F. C. Lee, "On a future for power electronics," *IEEE J. Emerg. Sel. Topics Power Electron.*, vol. 1, no. 2, pp. 59–72, Jun. 2013.
[22] G.-S. Seo, B.-H. Cho, and K.-C. Lee, "DC level dimmable LED driver using DC distribution," in *Proc. IEEE Energy Convers. Congr. Expo.*, Sep. 2013, pp. 4650–4654.
[23] L. L. Fernandes, E. S. Lee, D. L. DiBartolomeo, and A. McNeil, "Monitored lighting energy savings from dimmable lighting controls in The New York Times headquarters building," *Energy Buildings*, vol. 68, pp. 498–514, Jan. 2014.
[24] T. Dragicevic, J. M. Guerrero, and J. C. Vasquez, "A distributed control strategy for coordination of an autonomous LVDC microgrid based on power-line signaling," *IEEE Trans. Ind. Electron.*, vol. 61, no. 7, pp. 3313–3326, Jul. 2014.
[25] K. Lee, F. C. Lee, J. Wei, and M. Xu, "Analysis and design of adaptive bus voltage positioning system for two-stage voltage regulators," *IEEE Trans. Power Electron.*, vol. 24, no. 12, pp. 2735–2745, Dec. 2009.
[26] J. A. A. Qahouq and G. Muralidhar, "Control scheme for high-efficiency high-performance two-stage power converters," in *Proc. 24th Annu. IEEE Appl. Power Electron. Conf. Expo.*, Feb. 2009, pp. 1226–1232.
[27] C. P. Basso, *Switch-Mode Power Supplies: SPICE Simulations and Practical Designs*. New York, NY, USA: McGraw-Hill, 2008, pp. 579–670.
[28] R. W. Erickson and D. Maksimovic, *Fundamentals of Power Electronics*. Norwell, MA, USA: Kluwer, 2001, pp. 187–212.
[29] H. S. Athab, D. D.-C. Lu, and K. Ramar, "A single-switch AC/DC flyback converter using a CCM/DCM quasi-active power factor correction front-end," *IEEE Trans. Ind. Electron.*, vol. 59, no. 3, pp. 1517–1526, Mar. 2012.
[30] R. K. Singh and S. Mishra, "A magnetically coupled feedback-clamped optimal bidirectional battery charger," *IEEE Trans. Ind. Electron.*, vol. 60, no. 2, pp. 422–432, Feb. 2013.
[31] G.-S. Seo, J.-W. Shin, B.-H. Cho, and K.-C. Lee, "Digitally controlled current sensorless photovoltaic micro-converter for DC distribution," *IEEE Trans. Ind. Informat.*, vol. 10, no. 1, pp. 117–126, Feb. 2014.
[32] G. Spiazzi, D. Tagliavia, and S. Spampinato, "DC-DC flyback converters in the critical conduction mode: A re-examination," in *Proc. IEEE Ind. Appl. Conf.*, Oct. 2000, pp. 2426–2432.

Gab-Su Seo (S'10) received the B.S. degree from Chonnam National University, Gwangju, Korea, in 2008, and the M.S. degree in electrical engineering from Seoul National University, Seoul, Korea, in 2010, where he is currently pursuing the Ph.D. degree.

His current research interests include design, analysis, and control of photovoltaic power conditioning systems, dc distribution systems, integrated resonant converters, and low-profile power supplies.

Mr. Seo was a recipient of the Student Excellent Presentation Award at the First International Conference on Renewable Energy Research and Applications, Nagasaki, Japan, in 2012. He is a Student Member of the IEEE Power Electronics Society and the IEEE Industrial Electronics Society.

Hye-Jin Kim (S'12) received the B.S. and M.S. degrees in electrical engineering from Seoul National University, Seoul, Korea, in 2010 and 2012, respectively, where he is currently pursuing the Ph.D. degree.

His current research interests include design, analysis, and control of power factor correction converters, and distributed power systems.

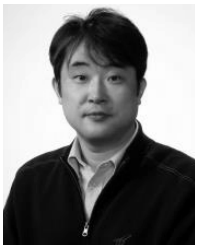

Kyu-Chan Lee (S'97–M'13) was born in Seoul, Korea, in 1964. He received the B.S., M.S., and Ph.D. degrees in electrical engineering from Seoul National University, Seoul, in 1987, 1989, and 2001, respectively.

He was a Research Engineer with Hyosung Industries Company, Ltd., Goyang, Korea, from 1989 to 1999, developing and designing power electronics systems, such as high-power converter and inverter systems. From 2000 to 2014, he was the Chief Executive Officer of Interpower Company, Ltd., Seoul. Since 2014, he has been the Chief Executive Officer of Smart Power Supply, Ltd., Seoul. His current research interests include developing and designing converter topologies and control methods for dc distribution systems, PV converter, and electronic ballast for metal halide discharge lamps.

Sung-Jin Choi (M'05) received the B.S., M.S., and Ph.D. degrees in electrical engineering from Seoul National University, Seoul, Korea, in 1996, 1998, and 2006, respectively.

He was a Research Engineer with Palabs Company, Ltd., Seoul, from 2006 to 2008. From 2008 to 2011, he was with Samsung Electronics Company, Ltd., Suwon, Korea, as a Senior and Principal Research Engineer, developing light-emitting diode drive circuits and wireless battery charging system. In 2011, he joined the University of Ulsan, Ulsan, Korea, where he is currently an Assistant Professor with the School of Electrical Engineering. His current research interests include component modeling, topology and control of high-frequency switching converters, and power electronics for renewable energy sources.

Bo-Hyung Cho (M'89–SM'95–F'11) received the B.S. and M.S. degrees from the California Institute of Technology, Pasadena, CA, USA, and the Ph.D. degree from the Virginia Polytechnic Institute and State University (Virginia Tech), Blacksburg, VA, USA, all in electrical engineering.

He was a member of the Technical Staff with the Department of Power Conversion Electronics, TRW Defense and Space System Group, prior to his research with Virginia Tech. From 1982 to 1995, he was a Professor with the Department of Electrical Engineering, Virginia Tech. In 1995, he joined the School of Electrical Engineering, Seoul National University, Seoul, Korea, where he is currently a Professor. His current research interests include power electronics, modeling, analysis, control of spacecraft power processing equipment, and distributed power systems.

Dr. Cho is a member of Tau Beta Pi. He was a recipient of the Presidential Young Investigator Award from the National Science Foundation in 1989. He was the Chair of the IEEE Power Electronics Specialists Conference in 2006.